OPERATIONAL DETERMINATION OF TIE POINTS AND BUNDLE ADJUSTMENT OF HRSC IMAGES OF THE MARS EXPRESS MISSION

R. Schmidt[a], *, M. Spiegel[b], C. Heipke[a], A. Dumke[b], G. Neukum[b] and the HRSC Co-Investigator Team

[a]Institute of Photogrammetry and GeoInformation, Leibniz Universität Hannover, Nienburger Str. 1, D-30167, Hannover, Germany - schmidt@ipi.uni-hannover.de
[b]Planetary Sciences and Remote Sensing, Freie Universität Berlin, Malteserstr. 74-100, D-12249 Berlin, Germany - michael.spiegel@mytum.de

Commission IV, WG IV/7

KEY WORDS: Extra-terrestrial, Adjustment, Matching, Orientation, Processing, Bundle, Three-Line, Planetary

ABSTRACT:

The pushbroom scanner HRSC (High Resolution Stereo Camera) onboard the European Mars Express mission is orbiting the planet Mars since January 2004 and delivers stereoscopic imagery with five panchromatic and four colour channels. This paper describes the process of improving the exterior orientation of the HRSC which is needed in order to derive high quality products such as high resolution Digital Terrain Models (DTMs) and ortho image mosaics from the data. The systematic photogrammetric processing for improving the exterior orientation is divided into two steps: First, a large number of tie points have to be automatically determined in the images using digital image matching. Second, a bundle adjustment is carried out using the globally available MOLA (Mars Orbiter Laser Altimeter) DTM as control information. The developed approaches of the matching and the bundle adjustment will be described in this paper. After that, the performance of both methods will be evaluated with respect to point accuracy and consistency with the MOLA DTM on the basis of 45 test data sets.

1. INTRODUCTION

Since January 2004 the HRSC (High Resolution Stereo Camera) onboard Mars Express is imaging the planet Mars stereoscopically, in colour and at high resolution and has returned more than 2300 image strips to earth. The pushbroom scanner, equipped with 9 CCD line detectors with 5176 pixels each mounted in parallel on the focal plane, is able to obtain panchromatic stereo data at three or five angles and colour data simultaneously in one image strip (Neukum et al. 2004). With an average flying height of about 270 km at pericenter a resolution of up to 12 m per pixel is achieved. The three-dimensional position of the orbiter with respect to the body-fixed coordinate system of Mars is permanently observed by Doppler measurements of the FDT (Flight Dynamics Team) of ESOC (European Space Operations Centre). The pose of the camera is adjusted with star trackers to the viewing direction from mission planning. The two elements position and pose form the exterior orientation of the HRSC with six values for each image line. An absolute accuracy of about 200 m is achieved in practice, but along flight direction the deviation can amount up to a few hundred meters. These values are not accurate enough for precise photogrammetric point determination. Therefore, a bundle adjustment is carried out to improve the relative accuracy of the ray intersections and the absolute position of the spacecraft. For absolute positioning the globally available MOLA (Mars Orbiter Laser Altimeter) DTM (Neumann et al. 2003) is used, which features high global accuracy and currently marks the best available reference system on Mars. With the improved exterior orientation high quality products such as high resolution DTMs or ortho image mosaics can be produced.

The improvement of the exterior orientation of the orbiter is divided into two separate steps: At first, a large number of tie points have to be determined automatically which will be used in the second step as input in the bundle adjustment. The automatic extraction of tie points is carried out at Institute of Photogrammetry and GeoInformation (IPI) of Leibniz Universität Hannover and the result is transferred to Photogrammetry and Remote Sensing (FPF) group of Technische Universität München respectively the Planetary Sciences and Remote Sensing group of Freie Universität Berlin.

Chapter 2 of this paper describes the process of automatically determining tie points in HRSC images. In chapter 3 the method of the bundle adjustment is explained. In chapter 4 the results of the single image strip processing are presented exemplified with 45 test orbits. The results of processing photogrammetric blocks are described in an accompanying paper (Dumke et al. 2008). Chapter 5 presents a short statistic of the results of the operational standard processing. The last chapter summarises the results and the conclusions are drawn.

2. DETERMINATION OF TIE POINTS

In this chapter the automatic determination of tie points is described. The general processing chain is displayed in Figure 1. The starting point are the radiometrically corrected HRSC images (called "level-2 images"). Because HRSC images often have a low signal-to-noise ratio an optional low pass filtering can be applied (cf. Gwinner et al. 2005). This step increases the robustness of the matching and the number of tie points. Extensive tests (Schmidt 2008) have shown that denoising algorithms like Anisotropic Diffusion (Perona & Malik 1990) or

---

* Corresponding author.

Non Local Means (Buades et al. 2005) are not able to yield advantage over a simple Gaussian. Only with stronger filtering the edge preserving nature of these algorithms becomes effective. However, for tie point extraction minimal filtering with a 3×3 pixel Gaussian window already generates on average about 50% more points compared to unfiltered images.
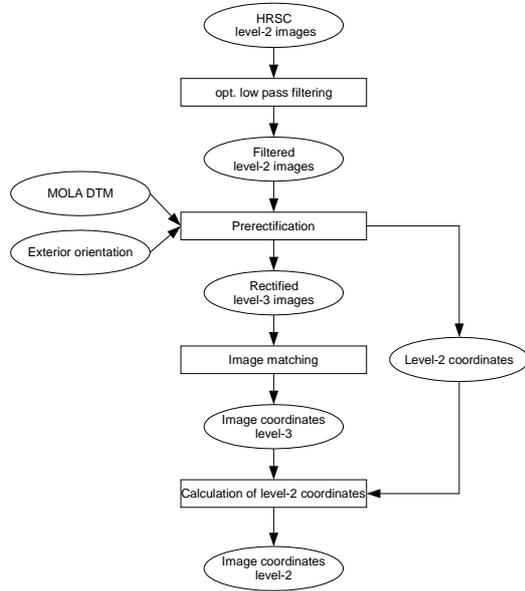

Figure 1. Processing chain of tie point extraction

In the next step the images are prerectified (Norvelle 1992, Scholten et al. 2005) using the exterior orientation provided by ESOC and the MOLA DTM. The resulting ortho photos (called "level-3 images") serve as input for the matching. The prerectification is necessary to compensate for scale differences caused by the elliptical orbit and for non-quadratic pixels caused by not perfectly adjusted integration times of the line scanner. As an example of the geometric differences which can occur a section from orbit 30 is shown in Figure 2:

Stereo 1 channel   Nadir channel   Stereo 2 channel
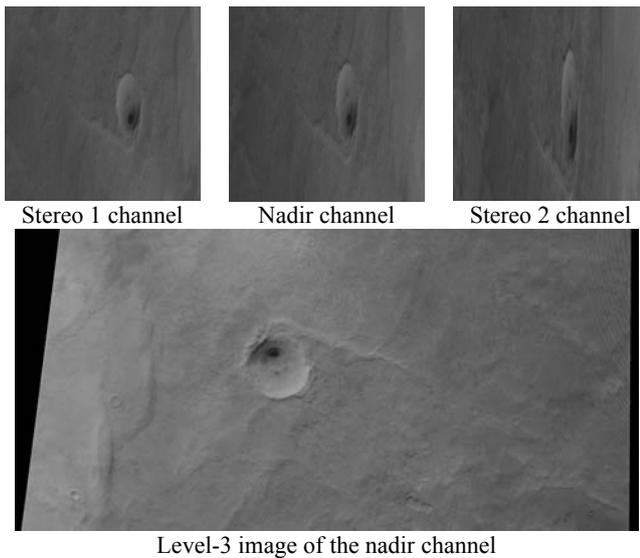
Level-3 image of the nadir channel

Figure 2. Geometric differences in images of the same strip

In the first row the crater is shown in the original level-2 images of the forward, nadir and backward looking channel. Underneath, the same area is shown in the rectified version of

the nadir channel. During rectification information about the origin of the level-3 pixels with respect to the level-2 images is stored in separate files (labelled "Level-2 coordinates" in Figure 1). After the matching this information is used to convert the level-3 image coordinates of the tie points back into the level-2 coordinate system of the original images where the collinearity equations used by the bundle adjustment are defined.

The matching employs a pyramidal approach to account for big parallaxes and imprecise approximate values of the exterior orientation. Generally, the nadir channel is matched pairwise with the remaining four panchromatic channels called stereo 1, stereo 2, photometry 1 and photometry 2. Additionally, it is possible to use the four colour channels blue, green, red and infrared if they are available at a decent resolution. Due to a low bandwidth between Earth and Mars for data transmission their resolution is often reduced via pixel binning (macro pixel). For example, a macro pixel format of 8×8 pixels decreases the size to 1/64th compared to the original amount of data which is inadequate for precise point determination.

The candidate points are distributed in a grid structure over the master image (nadir channel). Practical experience has shown that this approach is advantageous over a feature based operator with respect to HRSC data. This allows a more complete coverage with tie points and a more accurate adjustment of the point cloud to the MOLA DTM. An interest operator preferably generates points at edges which often coincide with breaklines in HRSC images. Because of the lower resolution of the MOLA dataset the differences to the HRSC points at these locations are higher than in flat terrain. Point transfer from the master image to the candidate image is carried out using the cartographic coordinates of the level-3 images.

The Normalised Cross-correlation Coefficient (NCC) is used as similarity measure which can compensate for radiometric differences with respect to gain and contrast. The NCC assumes parallel image and object planes without elevation differences in the correlation window. To a large extent this assumption is fulfilled in the prerectified images. Therefore, it is possible to use large correlation windows of 35×35 pixels or bigger which are needed to capture a sufficient number of grey value variations in low texture imagery.

To increase the accuracy of the points a multi-image least squares matching (MI-LSM) is carried out in which all points of a tuple are matched simultaneously. Following the approach of Krupnik & Schenk (1997) it is not necessary to estimate six affine transformation parameters per patch. As a result of the prerectification it is sufficient to estimate two horizontal translations only. The MI-LSM minimises the grey value differences between a particular image patch g^i, $i = 0, \ldots, n$ ($n+1$ = number of image patches) and the theoretical grey values of the surface patch (reference patch). Ideally the differences are zero but in reality errors occur because of radiometric and geometric inaccuracies:

$$\hat{G}(x, y) - g^i\left(x + d\hat{a}^i, y + d\hat{b}^i\right) = v(x, y) \qquad (1)$$

where

$\hat{G}(x, y)$ = theoretical grey values of reference patch
$g^i(x, y)$ = image patch grey values
$d\hat{a}^i, d\hat{b}^i$ = translations of patch i
v = residuals

For each pixel of the reference patch an equation can be formed in every image patch. The discretisation leads to the following linear system:

$$v = -g_x^i(x, y)d\hat{a}^i - g_y^i(x, y)d\hat{b}^i + d\hat{G}(x, y) \\ - g^i(x, y) + G_0(x, y) \tag{2}$$

where x, y = pixel coordinates
$g^i(x, y)$ = grey value of image patch i ($i = 1, \ldots, n$)
$g^0(x, y)$ = grey value of fixed image patch 0
g_x^i = grey value gradient with respect to x
g_y^i = grey value gradient with respect to y
$G_0(x, y)$ = initial value of theoretical grey value
$d\hat{a}^i, d\hat{b}^i$ = unknown translations of image patch i
$d\hat{G}(x, y)$ = unknown change of theor. grey value

To avoid a datum defect the position of the first image patch 0 has to be fixed, i.e. the translations are set to zero:

$$v = d\hat{G}(x, y) - g^0(x, y) + G_0(x, y) \tag{3}$$

With these two equations a Gauss-Markov model is set up and solved iteratively. The resulting final image coordinates are as already mentioned converted back to the level-2 coordinate system and serve as input for the subsequent bundle adjustment.

3. BUNDLE ADJUSTMENT

The bundle adjustment approach estimates the parameters of the exterior orientation only at few selected image lines, at the so-called orientation points. To fit the points obtained from the matching into the existing reference system on Mars the MOLA DTM is used as control information. Furthermore, the parameters of interior orientation have been improved by a similar bundle adjustment (Spiegel 2007a) and are assumed to be constant in the following approach.

The mathematical model for photogrammetric point determination with a three-line camera is a least squares adjustment and is based on the well known collinearity equations. In principle it is necessary to improve the exterior orientation parameters for each image line in which observed image coordinates are available. But, this is not possible due to geometric reasons. In case of Mars Express (satellite orbit) the trajectory is assumed to be stable and the parameters of the exterior orientation are improved only at few selected positions (orientation points). In order to obtain exterior orientation parameters for every sensor line the values lying in-between the orientation points are interpolated with Lagrange polynomials of grade three.

In case of Mars Express there are observed parameters of the exterior orientation for each image line. At the orientation points these observations can be introduced into the adjustment with additional observation equations. Because of Doppler shift measurements there are systematic effects in the observed exterior orientation. To model these effects in the bundle adjustment biases (offset) and drifts for the three position

parameters are used. For this, additional observation equations for bias and drift have to be introduced:

$$\hat{v}_{X_m} = \hat{X}_m - X_m + \hat{X}_B + j\hat{X}_D$$
$$\hat{v}_{Y_m} = \hat{Y}_m - Y_m + \hat{Y}_B + j\hat{Y}_D \tag{4}$$
$$\hat{v}_{Z_m} = \hat{Z}_m - Z_m + \hat{Z}_B + j\hat{Z}_D$$

where $\hat{v}_{X_m}, \hat{v}_{Y_m}..\hat{v}_{Z_m}$ = residuals at orientation points m
$\hat{X}_m, \hat{Y}_m, \hat{Z}_m$ = unknown ext. orientation parameters at orientation points
X_m, Y_m, Z_m = observed ext. orientation parameters at orientation points
$\hat{X}_B, \hat{Y}_B, \hat{Z}_B$ = unknown bias
$\hat{X}_D, \hat{Y}_D, \hat{Z}_D$ = unknown drift
j = number of image line

To use the MOLA DTM as control information the least squares adjustment has to be extended with an additional condition describing a relation between the MOLA DTM and the HRSC points. A bilinear surface defined by four neighbouring MOLA DTM M_i, $i = 1, \ldots, 4$ points is created for each HRSC point H (see Figure 3).
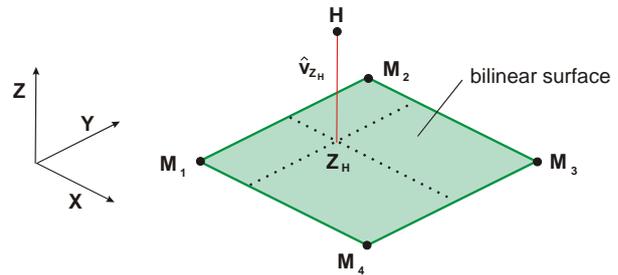

Figure 3. Fitting HRSC point in surface defined by MOLA

The condition that the HRSC points have to lie on these surfaces can be formulated as a constraint on the vertical distance from the HRSC point to the bilinear surface. Furthermore, this constraint can be substituted by a fictitious observation used as an additional observation in the bundle adjustment:

$$\hat{v}_{Z_H} = \hat{Z}_H - \left[\left(1 - \frac{\hat{X}_H - X_{M_1}}{d} \right) \left(1 - \frac{\hat{Y}_H - Y_{M_1}}{d} \right) Z_{M_1} \right.$$
$$+ \left(\frac{\hat{X}_H - X_{M_1}}{d} \right) \left(1 - \frac{\hat{Y}_H - Y_{M_1}}{d} \right) Z_{M_4}$$
$$+ \left(1 - \frac{\hat{X}_H - X_{M_1}}{d} \right) \left(\frac{\hat{Y}_H - Y_{M_1}}{d} \right) Z_{M_2}$$
$$\left. + \left(\frac{\hat{X}_H - X_{M_1}}{d} \right) \left(\frac{\hat{Y}_H - Y_{M_1}}{d} \right) Z_{M_3} \right] \tag{5}$$

where $\hat{v}_{Z_H}$ = residuals of height $\hat{Z}_H$

$\hat{Z}_H$ = unknown height of object point H

$\hat{X}_H , \hat{Y}_H$ = unknown coordinates of object point H

X_M , Y_M , Z_M = constant coordinates of MOLA DTM mesh point

d = Mesh width of MOLA DTM
$(d = X_{M_4} - X_{M_1} = Y_{M_2} - Y_{M_1})$

With this approach an improvement of the height (Z) can be expected. An improvement in planimetry (X, Y) can only be determined if there are different local terrain slopes at the MOLA surfaces. Figure 4 demonstrates a situation before bundle adjustment:
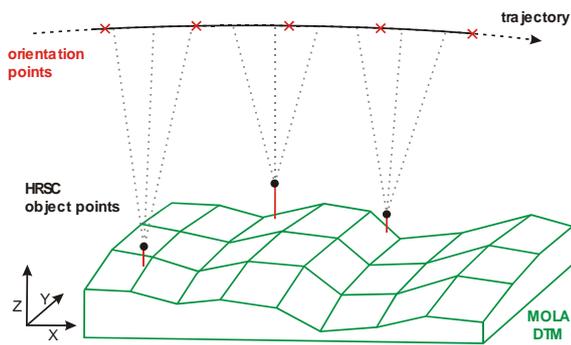

Figure 4. Situation before bundle adjustment

After bundle adjustment the differences (red lines) between HRSC points and MOLA DTM are reduced (see Figure 5):
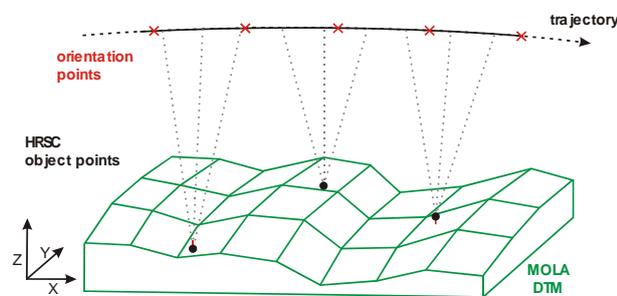

Figure 5. Situation after bundle adjustment

The adjustment can be divided into two steps which are called Relative and Absolute Orientation here: In the first part the ray intersections are improved by estimating the pitch and yaw angles at the orientation points. For geometric reasons the roll angle can only be determined with poor accuracy. In this step points are eliminated which are considered erroneous on the basis of their residuals of the image coordinates. In the second part the point cloud is adjusted to the MOLA DTM for absolute positioning. For that purpose biases for the three parameters of position and one drift for the height component are estimated. The angles are determined at the orientation points like in the first step. Additionally, the roll angle is calculated which was not possible in the first step.

For the stochastic model the observed image coordinates are considered to be uncorrelated and with equal accuracy. For estimation of the Absolute Orientation the stochastic model is altered that the ray intersections from the Relative Orientation are kept unchanged. Only translations, a tilting in the height component and the roll angle are effectively carried out. Also in this step HRSC points are eliminated by taking into account the differences between the HRSC and the MOLA points. Single HRSC points are eliminated which exhibit major residuals to the MOLA DTM. Generally, these are no errors from matching but points which are not visible in the MOLA dataset because of its lower resolution (e.g. small craters). The bundle adjustment approach is described in more detail in Spiegel (2007a) and Spiegel (2007b).

4. RESULTS

In order to evaluate the developed approach results are presented which are obtained from a test dataset of 45 chosen test orbits. Image quality varies from very good to images whose contrast and sharpness have been blurred by dust in the atmosphere. All kinds of topography is contained in the data set: diverse landscapes with many craters, areas of erosion and textureless regions. Valley networks with steep and hillsides with continuous height changes can be found. The resolution of the prerectified images varies from 13 m to 60 m.

The ray intersections of the matching points are evaluated with a bundle adjustment for all 45 test orbits. In addition to the scheme of chapter 3 the accuracy of the a priori image coordinates is adapted in an iterative way. The bundle adjustment is repeated until a value of 1.0 is obtained for the standard deviation of the weights σ_0. This assures that the standard deviations of different orbits are comparable with each other. Figure 6–8 show the standard deviations of the ray intersections for all 45 test orbits before and after bundle adjustment. The values apply to a local coordinate system where X (along flying direction) and Y (across flying direction) indicate the horizontal position and Z the height component.
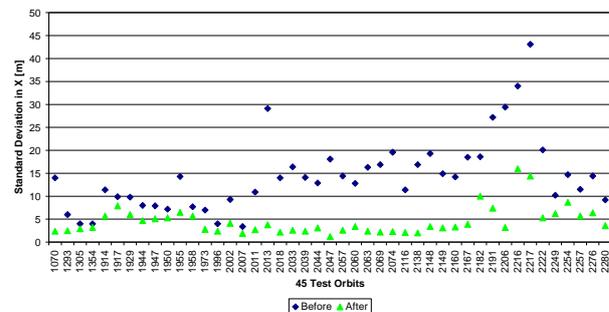

Figure 6: Standard deviations [m] of the ray intersections for all 45 test orbits in X (along flying direction) before and after BA
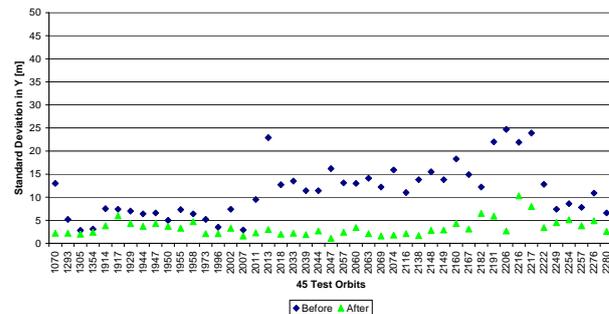

Figure 7: Standard deviations [m] of the ray intersections for all 45 test orbits in Y (across flying direction) before and after BA
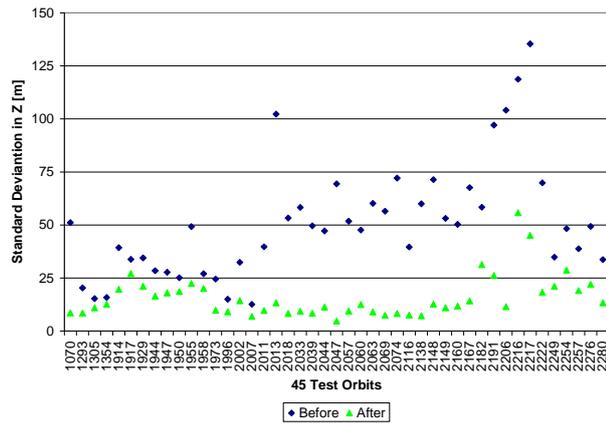
Figure 8: Standard deviations [m] of the ray intersections for all 45 test orbits in Z (height component) before and after BA

Table 1 shows the standard deviations of the ray intersections averaged over all 45 test orbits. The respective left column shows the value before adjustment using the nominal exterior orientation. The right column shows the result of the bundle adjustment (labelled "BA"). Results for Cross Correlation only and LSM are given.

Method	X	X_{BA}	Y	Y_{BA}	Z	Z_{BA}
CC	15.6	7.3	12.2	5.5	55.5	25.6
LSM	14.5	4.5	11.3	3.4	50.9	15.8

Table 1. Standard deviations [m] of the ray intersections averaged over all 45 test orbits

Due to a small convergence angle of the HRSC the height component cannot be determined as precisely as planimetry. Before bundle adjustment the points derived from LSM are slightly more accurate. The points derived from CC can be improved by a factor of 2.2 by bundle adjustment whereas the points derived from LSM have been improved by a factor of 3.2. With respect to an average resolution of 30 m of the prerectified images a very high accuracy has been achieved. In the next table the a posteriori standard deviations of the image coordinates and the percentage of rays of the tuples have been verified:

Method	Accuracy of image coordinates	2-ray [%]	3-ray [%]	4-ray [%]	5-ray [%]
CC	0.32	8.0	9.6	8.7	73.7
LSM	0.19	8.5	9.6	8.4	73.5

Table 2. A posteriori standard deviations [pixel] of the image coordinates and the percentage of rays of the tuples averaged over all 45 test orbits

It can be seen that with CC a high accuracy of 1/3 pixel has been attained. With LSM an increased accuracy of 1/5 pixel has been achieved. For a stable bundle adjustment a high percentage of 5-ray points is desirable and the percentage of 2-ray points should be as small as possible because they are omitted in the bundle adjustment. About 3/4 of all tuples consist of all five rays and the remaining values are below 10%. This means that matching delivers rather strong geometric blocks. Finally, it should be noted that the percentage of

blunders is about 10% including the points eliminated which do not fit to MOLA and that 10 000-60 000 points per strip have been found.

Next, in the second step the HRSC object points are tied to the MOLA DTM. For this task, the a priori accuracy of the exterior orientation has been introduced into the bundle adjustment with a value of 1000 m for the position and 25 mdeg for the attitude at the orientation points. The MOLA DTM is introduced with an accuracy of 100 m in order to cope with differences between HRSC object points and MOLA track points due to the limited spatial resolution of MOLA. As mentioned before, the resolution on the ground of HRSC is up to 12 m compared to the MOLA surface footprint of about 168 m. Regarding local areas, the MOLA data describe the surface less detailed as HRSC object points.

The root-mean-square (RMS) differences between the HRSC and the MOLA DTM is reduced significantly in the bundle adjustment. Hence, there is a high consistency between HRSC points and the MOLA reference system after the bundle adjustment. This is clearly visible in Figure 9 which shows the height differences between the HRSC object points and the MOLA DTM of orbit 2063 before and after bundle adjustment.
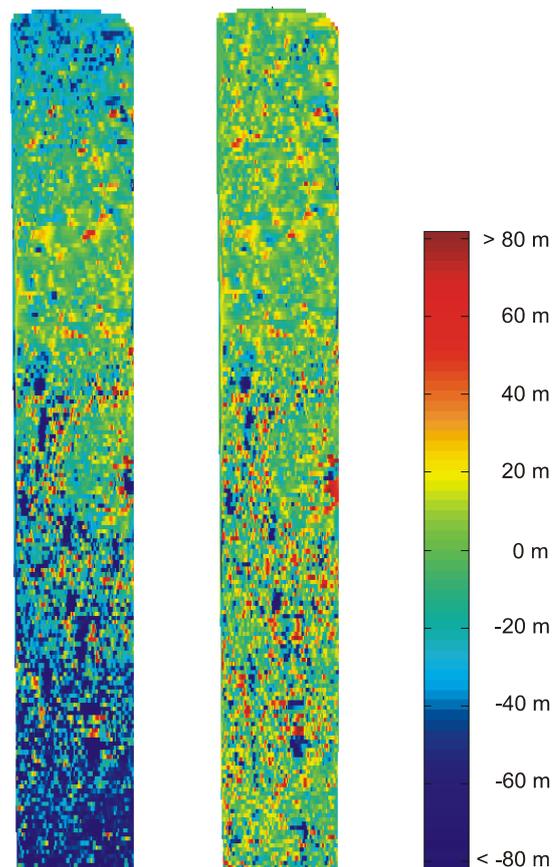

Figure 9: Height differences between HRSC object points and MOLA DTM of orbit 2063 before bundle adjustment (left), and after bundle adjustment (right)

In Figure 10 statistics for all investigated 45 test orbits are shown. As can be seen, the height differences between HRSC object points and MOLA DTM is reduced for all 45 investigated orbits on average by a factor of 1.5.
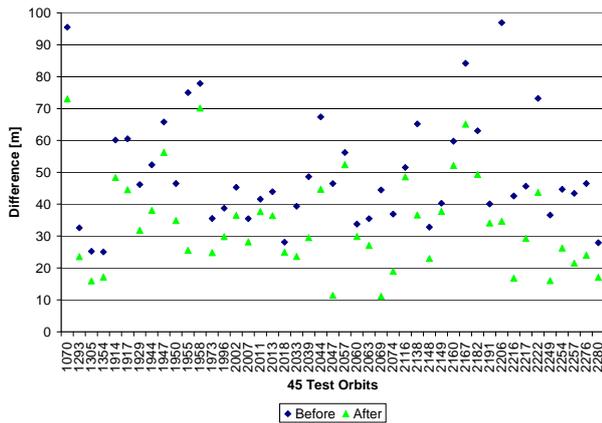
Figure 10: Height differences between HRSC object points and MOLA DTM before and after bundle adjustment

5. OPERATIONAL PROCESSING OF ALL HRSC IMAGERY

So far, the data of the first 5000 orbits of Mars Express have been processed in the desrcibed way, i.e. until orbit h4995_0001 which was recorded in November 2007. During this time about 1900 image strips of the surface of Mars have been received. Because of dust storms, low texture, data gaps, limb images, overexposed images or too short image strips only 1396 orbits are usable for a photogrammetric point determination. Successfully registered to the MOLA DTM are 1138 orbits (=82%); the reasons for failure are bad image quality or flat terrain. In the case of flat terrain the used method for absolute orientation allows registration to MOLA in height but not in horizontal direction.

6. CONCLUSIONS

It has been shown that the tie points have on average a very high accuracy of 4.5 m in X (along flying direction), 3.4 m in Y (across flying direction) and 15.8 m in Z (height component). These values have to be seen in context with the fact that the average resolution of the prerectified images is 30 m. The image coordinates have an accuracy of 1/5 pixel with LSM which is a very good value considering the difficult image data. Depending on the size of the image strips between 10 000 and 60 000 tie points have been found which is sufficient for a stable Relative and Absolute Orientation. About 75% of these tuples comprise all five rays.

Before using bundle adjustment the height differences between the HRSC object points and the MOLA DTM show a systematic curvature. After improving the orbits with bundle adjustment the height differences between the HRSC object points and the MOLA DTM are reduced for all 1138 successfully computed orbits. Thus, the approach reaches a high consistency between HRSC points and MOLA DTM, which constitutes the currently best reference system on Mars.

REFERENCES

Buades, A., Coll, B., Morel, J. M., 2005. A Review of Image Denoising Algorithms with a New One. *Multiscale Modeling & Simulation*, 4 (2), pp. 490–530.

Dumke, A., Spiegel, M., Schmidt, R., 2008. Mars: High-Resolution Digital Terrain Model and Ortho-Image Mosaic on the Basis of MEX/HRSC Data. *IntArchPhRS*, 37 (4), this congress.

Gwinner, K., Scholten, F., Giese, B., Oberst, J., Jaumann, R., Spiegel, M., Schmidt, R., Neukum, G., 2005. Hochauflösende Digitale Geländemodelle auf der Grundlage von Mars Express HRSC-Daten. *Photogrammetrie Fernerkundung Geoinformation*, 5/2005, pp. 387–394.

Krupnik, A., Schenk, T., 1997. Experiments with matching in the object space for aerotriangulation, *ISPRS Journal of Photogrammetry and Remote Sensing*, 52 (4), pp. 160–168.

Neukum, G., Jaumann, R., HRSC Co-Investigator and Experiment Team, 2004. HRSC: The High Resolution Stereo Camera of Mars Express. In: Mars Express: the scientific payload, Andrew Wilson (Ed.), scientific coordination: Agustin Chicarro, ESA SP-1240, Noordwijk, Netherlands: ESA Publications Division, ISBN 92-9092-556-6, pp. 17–35.

Neumann, G., Lemoine, F., Smith, D. and Zuber, M., 2003. The Mars Orbiter Laser Altimeter Archive: Final Precision Experiment Data Record Release and Status of Radiometry. In: Lunar and Planetary Science XXXIV, Abstract #1978, Lunar and Planetary Institute, Houston.

Norvelle, F. R., 1992. Stereo Correlation: Window Shaping and DEM Corrections. *PE&RS*, 58 (1), pp. 111–115.

Perona, P., Malik, J., 1990. Scale-Space and Edge Detection using Anisotropic Diffusion. *IEEE Trans. on Pattern Analysis and Machine Intelligence*, 12 (7), pp. 629–639.

Schmidt, R., 2008. Automatische Bestimmung von Verknüpfungspunkten für HRSC-Bilder der Mars Express-Mission. Dissertation, Leibniz Universität Hannover, submitted.

Scholten, F., Gwinner, K., Roatsch, T., Matz, K.-D., Wählisch, M., Giese, B., Oberst, J., Jaumann, R., Neukum, G., 2005. Mars Express HRSC Data Processing – Methods and Operational Aspects. *PE&RS*, 71 (10), pp. 1143–1152.

Spiegel, M., 2007a. Improvement of Interior and Exterior Orientation of the Three Line Camera HRSC with a Simultaneous Adjustment. *IntArchPhRS*, 36 (3/W49B), pp. 161–166.

Spiegel, M., 2007b. Kombinierte Ausgleichung der Mars Express HRSC Zeilenbilddaten und des Mars Global Surveyor MOLA DGM. Dissertation, DGK C, 610, Verlag der Bayerischen Akademie der Wissenschaften, München, http://129.187.165.2/typo3_dgk/docs/c-610.pdf.